

# Microscopic theory of warm ionized gases: equation of state and kinetic Schottky anomaly

A Capolupo, S M Giampaolo, F Illuminati

Dipartimento di Ingegneria Industriale, Università di Salerno, Via Ponte don Melillo, I-84084 Fisciano (SA), Italy

**Abstract.** Based on accurate Lennard-Jones type interaction potentials, we derive a closed set of state equations for the description of warm atomic gases in the presence of ionization processes. The specific heat is predicted to exhibit peaks in correspondence to single and multiple ionizations. Such kinetic analogue in atomic gases of the Schottky anomaly in solids is enhanced at intermediate and low atomic densities. The case of adiabatic compression of noble gases is analyzed in detail and the implications on sonoluminescence are discussed.

## 1. Introduction

The recent progresses in stellar astrophysics [1]–[3], in experiments on inertial confinement in plasmas [4]–[6], and in plasma diagnostics have triggered renewed interest in the determination of accurate state equations for mixed systems of atoms and ions in ionized gases [7, 8, 9]. At the same time, much recent effort has been devoted to investigating the role of plasmas of ionized atomic gases in sonoluminescence (SL) [10]–[19]. Sonoluminescence consists in the emission of short flashes of light from collapsing bubbles in a liquid excited by ultrasonic waves. The light-emitting bubbles contain mainly noble gas atoms plus small quantities of water vapor and in the last part of the collapse they can reach densities comparable to those of solids. According to recent results [19] the conditions inside the bubbles may be very extreme, the temperature may far exceed those estimated from the emitted light, and the plasma electron density can reach the same order of magnitude as that of densities created in laser-driven fusion experiments. A detailed understanding of the noble-gas thermodynamics in the high energy regime is then crucial in order to explain the experimental results and uncover the basic mechanisms of sonoluminescence.

In the present work we analyze the thermodynamics of atomic gases for different regimes of atomic densities and temperatures characteristic of warm plasmas, and consider applications to the case of noble gases by studying regimes that can be typical of the last stage of collapsing bubbles in sonoluminescence, i.e. the stage of light emission. We derive a set of state equations based on accurate microscopic interaction potentials of the Lennard-Jones type and we predict the presence of anomalous peaks in the specific heats. These peaks are explained in terms of a kinetic extension of the Schottky anomaly observed in solids with a limited number of energy levels at very low temperature [20]. The peaks appear in correspondence to ionization processes as the temperature is increased. This implies that the different degrees of ionization play in plasma physics a role similar to the one played by the finite number of energy levels in the solid state case, the fundamental difference lying in the fact that the predicted nontrivial contribution



to the specific heat in ionized gases is provided by the unbounded nature of the atomic kinetic energy. The existence of kinetic Schottky anomalies bears important consequences on the collective heating of atomic gases. In particular, it is strongly suppressed when the specific heats undergo a sharp increase in correspondence of atomic ionizations. Coming to concrete settings, we will discuss in detail the case of noble gases, which is especially relevant for sonoluminescence. Considering the late stage of adiabatic compression, we determine self-consistently the number density of plasma electrons and find good agreement with recently reported experimental results [19]. Finally, we remark that our approach can be readily generalized beyond the case of atomic gases by including in the description the presence of chemical bonds.

The paper is organized as follows. In the Sec. 2 we define a set of state equations useful for warm plasmas, and we analyze the ultra-low density and the high density plasma regimes in Secs. 3 and 4, respectively. In Sec. 5 we consider an adiabatic transformation and compare the results obtained by using the state equations introduced in Sec. 2 with new experimental data on the sonoluminescence. Sec. 6 is devoted to the conclusions.

## 2. Equations of state

We begin by introducing the constitutive equations for the energy of a generic particle system in the presence of ionization. By taking into account the kinetic, interaction, and ionization contributions, the energy density of the atomic ensemble can be expressed as

$$E = \frac{3}{2}K_bT \sum_{i=-1}^{N_A} n_i + \sum_{i=-1}^{N_A} n_i(E_i + h_i), \quad (1)$$

where the index  $i$  classifies the particles present in the systems (electrons, atoms, and ions of different charge multiplicity) by their charge expressed in units of  $|e|$ . Explicitly,  $i = -1$  for free electrons,  $i = 0$  for neutral atom and  $i \in [1, N_A]$  for ions of different charge, ranging up to the maximum allowed value corresponding to the atomic number  $N_A$ . The number density of the  $i$ -th particle species is denoted by  $n_i$ , while  $E_i$  is the energy needed to ionize an atom  $i$  times, with  $E_{-1} = E_0 = 0$ . Finally,  $h_i$  is the potential energy density of the  $i$ -th particle species due to the interaction with the other particles of the system. Taking the virial expansion up to second order (higher orders may be considered when necessary),  $h_i$  takes the form

$$h_i = \sum_{j=-1}^{N_A} 2\pi n_j \int_0^\infty r^2 U_{i,j}(r) \exp\left(-\frac{U_{i,j}(r)}{K_bT}\right) dr, \quad (2)$$

where  $U_{i,j}(r)$  is the interaction energy between the  $i$ -th and the  $j$ -th particles at distance  $r$ . In Eq. (1) we have neglected the presence of chemical bonds between the atoms. Such assumption holds, for instance, in the case of noble gas atoms. The approach can be readily extended to other systems by taking into account the energy associated to the chemical bond.

The atom and ion densities  $n_i$  are not fixed *a priori*, but are determined by the underlying quantum dynamics through the self-consistent coupling of Eq. (2) and the Saha equations [21]:

$$\frac{n_{i+1} n_{-1}}{n_i} = \left(\frac{m_e K_b T}{2\pi \hbar^2}\right)^{\frac{3}{2}} \frac{2g_{i+1} e^{-\frac{E_{i+1} + h_{i+1} + h_{-1}}{K_b T}}}{g_i e^{-\frac{E_i + h_i}{K_b T}}}, \quad (3)$$

where  $m_e$  is the electron mass and  $g_i$  is the ground-state degeneracy of an atom ionized  $i$ -th times. Eq. (3) is a set of  $N_A$  equations in  $N_A + 2$  variables represented by the densities  $n_i$ . This set of equations can be closed by taking into account that the electronic density is related

to the ion density by  $n_{-1} = \sum_{i=1}^{N_A} in_i$  and that  $n_0$  is related to the total atomic density  $n$  by  $n_0 = n - \sum_{i=1}^{N_A} n_i$ .

We now provide an expression for the pressure  $P$ . In agreement with Eq. (1),  $P$  can be written as the sum of a kinetic term and a term associated to the interaction of any particle with the surrounding ones,

$$P = K_b T \sum_{i=-1}^{N_A} n_i - 2\pi \sum_{i=-1}^{N_A} n_i h'_i, \quad (4)$$

where the interaction term  $h'_i$ , considering the virial expansion up to second order, reads

$$h'_i = \sum_{j=-1}^{N_A} n_j \int_0^\infty r^3 \frac{dU_{i,j}(r)}{dr} \exp\left(-\frac{U_{i,j}(r)}{K_b T}\right) dr. \quad (5)$$

By means of Eq. (1) we can compute the specific heat at constant volume,  $c_v = \left(\frac{\partial E}{\partial T}\right)_V$ . Eq. (4) can be used to obtain the specific heat at constant pressure by using the relation  $c_p - c_v = -T \left(\frac{\partial P}{\partial V}\right)_T^{-1} \left(\frac{\partial P}{\partial T}\right)_V^2$ .

Eqs.(1)–(5) identify a complete set of state equations for a gas in which the degree of ionization is determined self-consistently from thermal equilibrium. In the following we will apply such equations to the description of warm plasmas.

### 3. Non interacting models: warm plasma at low density

We consider first ultra-low density regimes such that the interaction effects can be neglected, i.e. we can put ( $U_{i,j} = 0, \forall i, j$ ).

The main outcomes are presented in Figs. 1 and 2 in which the dependence of  $P$ ,  $c_v$  and  $c_p$ , as well as the dependence of free electron density  $n_{-1}$  on the temperature are shown for different densities of a system of Helium atoms.

Let us start from the top panel of both the figures, which refers to an extremely low total density  $n = 10^{10} \text{cm}^{-3}$ . In Fig. 1 we note the presence of two peaks in both the specific heats in correspondence of the two different ionization processes, which are signaled by steps in the free-electron density  $n_{-1}$ . In Fig. 2 the pressure shows a step-wise behavior associated to the increment of free-electrons released in the ionization process.

Comparing now the top panel with the central one, in which the density is higher, we may observe that the peaks of the specific heats becomes lower, and the step-wise shapes of  $n_{-1}$  and  $P$  are wider and less pronounced. This is due to the fact that the ranges of temperature in which the processes of first and second ionization occur start to merge together. The smoothing of the steps continues up to the step-wise shape disappears almost completely when the density approaches to values comparable with those typical of metals (bottom panel  $n = 10^{22} \text{cm}^{-3}$ ).

The peculiar behavior of the specific heats can be explained, as in the Schottky anomaly case, by taking into account the ratio of the change of the system entropy. For temperatures relatively low with respect to the one at which ionizations become relevant, the entropy of the system is small because all the atoms are in the same state. As the temperature approaches the difference between the energy levels, the different ionization states become significantly populated and hence there is an enormous increment of the system entropy due to the uncertainty on the degree of ionization. This implies the presence of peaks in the profiles of the specific heats. At the difference of the Schottky anomaly in the solid state physics, in the plasma case the entropies are related also to the kinetic energy of the atoms.

### 4. Interacting models: warm dense plasma

We now take into account the interactions between different particles by introducing potentials  $U_{i,j}$  which can describe the physics of warm dense plasmas.

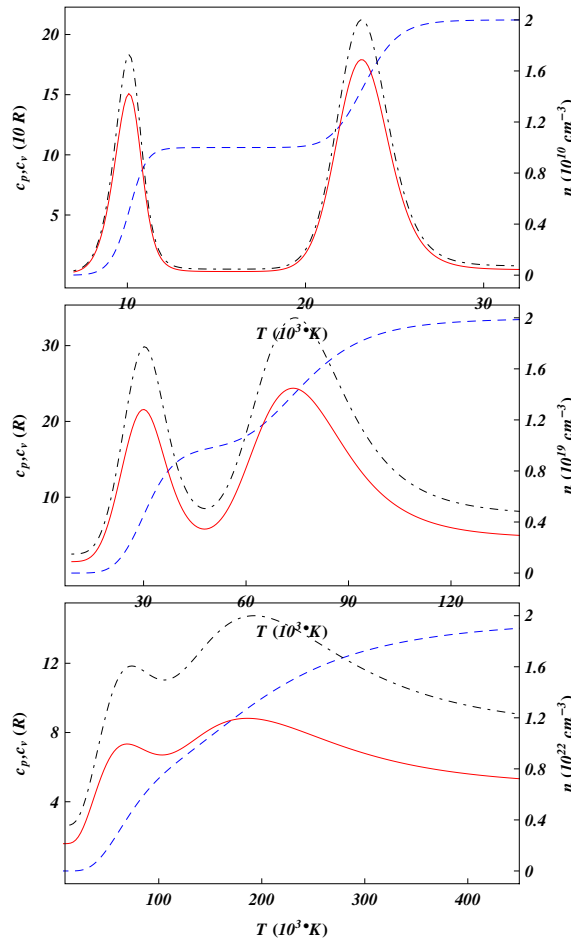


**Figure 1.** Dependence of the molar specific heat at constant volume  $c_v$  (Red solid line), and at constant pressure  $c_p$  (black dot-dashed line) on the temperature compared with the electron density  $n_{-1}$  (blue dashed line) for an ensemble of Helium atoms at three different densities  $n$ . In top panel  $n = 10^{10} \text{ cm}^{-3}$ , in central panel  $n = 10^{19} \text{ cm}^{-3}$ , and in bottom panel  $n = 10^{22} \text{ cm}^{-3}$ . Both the specific heats are expressed as function of the universal constant of gas  $R$  in order to simplify their comparison with the result obtained with different assumptions.

Let us start by assuming that the interaction between two neutral atoms of noble gas can be represented by Lennard-Jones potential  $U_{0,0}(r) = 4\epsilon \left[ \left( \frac{\sigma}{r} \right)^{12} - \left( \frac{\sigma}{r} \right)^6 \right]$  in which  $\epsilon$  stands for the depth of the potential well and  $\sigma$  is the finite distance at which the inter-particle potential vanishes. Lennard-Jones potential can be seen as the sum of two terms of which the first one is repulsive and represents the short range Pauli repulsion due to the partial overlap of the electron clouds of the two atoms, while the second one represents the long range dipole-dipole attraction. The interaction energy between a neutral atom and an ion can be represented by adding to  $U_{0,0}$  the charge-dipole attractions  $U_{0,i}(r) = U_{0,0}(r) - i^2 \alpha E_i^2(r)$ , where  $\alpha$  is the polarizability of the neutral atom and  $E_i(r)$  is the electric field associated to the electrostatic potential  $W_i(r)$  that solve the Debye-Hückel equation [21]. In a similar way, we describe ion-ion interaction by adding to the standard Lennard-Jones term both the charge-dipole interactions and the electrostatic repulsion between charges,  $U_{i,j}(r) = U_{0,0}(r) - (i^2 + j^2) \alpha E_i^2(r) + ijW_i(r)$ .

The interaction involving one or two free-electrons can be described by considering any free

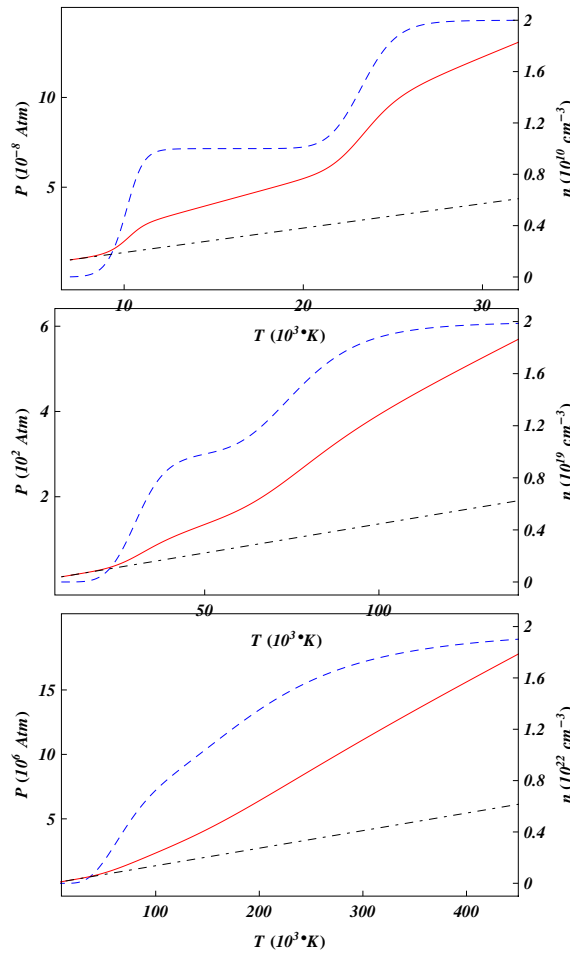


**Figure 2.** Dependence of the pressure (red line) on the temperature compared with the electron density  $n_{-1}$  (blue dashed line) and with the pressure obtained from the ideal gas law neglecting the ionization (black dot-dashed line) for an ensemble of atoms of Helium at the same three different densities showed in Fig. 1.

electron as a cloud similar to the one surrounding an Hydrogen atom, but with a radius equal to the thermal De Broglie length  $\lambda$  and a polarizability equal to 0. With these assumptions free-electrons have interactions similar to the ionic ones. Indeed, the interaction terms between a free-electron and an ion can be described by replacing in the Lennard Jones term,  $\sigma$  with  $\frac{\sigma+\lambda}{2}$  and  $\varepsilon$  with  $\sqrt{\varepsilon\varepsilon_H}$  (being  $\varepsilon_H$  the depth of the potential well of the Lennard-Jones potentials between two atoms of Hydrogen), and the  $U_{-1,-1}(r)$  term can be represented by substituting  $\sigma$  with  $\lambda$  and  $\varepsilon$  with  $\varepsilon_H$ .

In order to show the difference of behavior between the dense interacting and the non-interacting plasmas we consider a system of Xenon atoms at high density and neglect the dependence of  $\sigma$  and  $\varepsilon$  on the degree of ionization. This approximation does not affect the results in the case in which only of the first ionizations are considered. The plots in Fig. 3 are obtained by considering the first two degrees of ionization of the Xenon and  $n = 10^{22} \text{cm}^{-3}$ . Such plots show that the presence of particle interactions in the state equations does not change significantly the value of  $c_v$ , even at high densities. Indeed, the fields  $h_i$  in Eq. (2) are about an order of magnitude lower than the ionization energy and therefore their effects on the solution of Saha Equation Eq. (3) are almost negligible. On the contrary, the behaviors of  $P$  and of  $c_p$

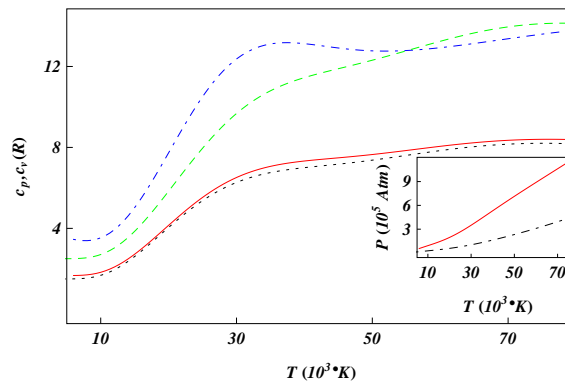


**Figure 3.** Comparison between interacting and non interacting cases for a mole of xenon. In the main plot it is shown the comparison between the specific heats. Dotted black line stands for  $c_v$  in the non interacting case, and solid red line shows  $c_v$  in the interacting framework. Green dashed line denotes  $c_p$  in the non interacting case, and Blue dot-dashed line represents  $c_p$  in the interacting case. In the inset we present the comparison between the pressures. Black dot dashed line refers to the pressure in the non interacting case while the red solid line shows the same quantity in the interacting framework. We considered  $n = 10^{22} \text{ cm}^{-3}$  and only the first two degrees of ionization.

are strongly influenced by the interactions.

### 5. Adiabatic compression and Schottky like anomaly

In this section we show the influence of the Schottky like anomaly on the temperature in an adiabatic compression. We consider such particular transformation because it plays a fundamental role in different phenomena as for example in the sonoluminescence. Indeed, in such phenomenon the gas inside the bubble follows an isothermal transformation in the bubble expansion phase and an adiabatic compression during the bubble collapse, which represents the more characterizing phase for the emission of light [13].

We study in particular a quasi-static adiabatic compression of a sphere containing 1 mole of atoms which is initially in thermal equilibrium under the standard conditions of pressure and temperature ( $P = 1 \text{ atm}$ ,  $T = 300^\circ K$ ), and assume that the compression stops when the density in the sphere becomes comparable with the one present in sonoluminescing bubble during the last part of the collapse.

The results of our evaluation are displayed in Fig. 4. Notice that when the radius of the sphere  $R$  is large, the solutions obtained for an ideal gas are indistinguishable from our ones. When  $R$  becomes smaller than  $0.2 R_a$  ( $R_a \simeq 18.04 \text{ cm}$  stands for the radius of sphere at standard condition), gas temperatures obtained by our state equations are lower than the ones obtained for ideal gas. The lowering of the temperature, that depends on the kind of atoms in the sphere, is due to the fact that a part of the energy provided to the system by the compression is used by some atoms to ionize themselves. Atoms of Xenon are the ones in which this effect is more relevant because their ionization energies are lower than the ones of the Argon and of the Helium. Hence the ionization process becomes relevant at higher radii (lower temperatures). Even if the number of free-electrons is very low compared to the number of the atoms, and hence we are only at the onset of the Schottky anomaly, the effect is so strong to halve the temperature in the Helium case at  $R = 0.05 R_a$ . The correction is even stronger if we compare our results with the temperature obtained for van der Waals gases which diverges when the volume of the bubble approaches the covolume of the species.

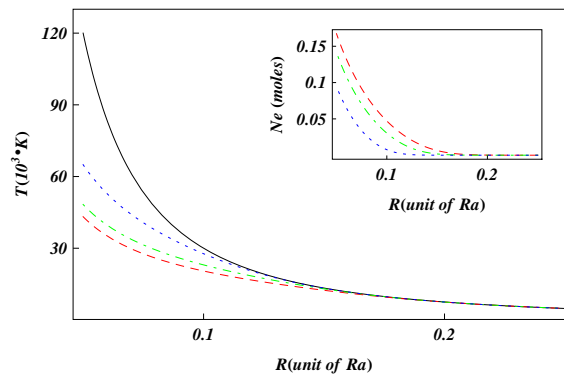


**Figure 4.** Main plot: Dependence of the temperature on the bubble radius (expressed in unit of the ambient radius  $R_a$ ), in the case of an adiabatic compression, for the ideal gas (black line) compared with the one that we have obtained using our set of state equations for Helium (blue dotted line), Argon (green dot-dashed line) and Xenon (red dashed-line). Inset: total number of free-electrons as function of the the bubble radius, in the case of an adiabatic compression for the same atomic species of the main plot.

Finally, we note that for densities comparable with the one present in sonoluminescing bubble, the electronic density is in good agreement with the recent results on sonoluminescence [19] according to which the plasma electron density in the bubble exceeds  $10^{21} \text{ cm}^{-3}$ . In a forthcoming paper we will analyze in detail the dynamic of sonoluminescing bubbles.

## 6. Conclusions

We have presented a set of state equations useful for plasma physics, in which the ionization degrees are not fixed *a priori* but are obtained self-consistently using the Saha equation. We derive state equations that can describe thermodynamical properties of warm plasmas both with low and high density. We have focused our analysis on the noble gas atoms, because of their importance in many physical phenomena such as sonoluminescence, but our work can be easily extended also to all kinds of atoms, molecules and mixtures of them by considering also chemical bounds. Using this new approach, we revealed a Schottky like anomaly in the specific heats of noble gas atoms at low densities, and a step-wise behavior of pressure and density of the free-electrons associated to ionization processes.

The anomalies in specific heats become less evident at high densities and disappear when all the atoms are fully ionized. Such anomalies can play a very relevant role in many phenomena of actual interest as for example in sonoluminescence in which collapsing bubbles close to their minimum radius reach temperatures of few tens of thousands of  $K$ , densities of order of the solid one and are almost completely filled with noble gas atoms [13, 14]. In such phenomenon, during the last part of the collapse phase, the temperature and the radial speed of the bubble depend on  $c_p$  and  $c_v$ , then an increment of them can influence strongly the bubble dynamic. In the present paper we have not directly considered the problem of the dynamic of sonoluminescence, which will be analyzed in detail elsewhere, but we have only treated the simple problem of an adiabatic compression of a sphere that reaches a final density comparable with the one of sonoluminescence during the emission. However, even with this simple dynamic, we have obtained electronic densities for the gas in the sphere which is in good agreement with some recent experimental results on sonoluminescence.

## Acknowledgement

We acknowledge financial support from the European Commission of the European Union under the FP7 STREP Project HIP (Hybrid Information Processing), Grant Agreement n. 221889.

## References

- [1] Guillot T 1999 *Science* **286** 72
- [2] Remington B A, Drake R P and Ryutov D D 2006 *Rev. Mod. Phys.* **78** 755
- [3] Van Horn H M 1991 *Science* **252** 384
- [4] Koenig M et al. 2005 *Plasma Phys. Contr. Fusion* **47** B441
- [5] Atzeni S and Meyer-ter-Vehn J 2004 *The Physics of Inertial Fusion*, Clarendon Press, Oxford
- [6] Key M H 2007 *Phys. Plasmas* **14** 055502
- [7] Hummer D G and Mihalas D 1988 *Astroph. J.* **331** 794
- [8] Rogers F J, Swenson F J, and Iglesias C A 1996 *Astroph. J.* **456** 902
- [9] Cardona O, Martinez-Arroyo M, and Lopez-Castillo M A 2010 *Astroph. J.* **711** 239
- [10] Barber B P and Putterman S J 1991 *Nature* **352** 318
- [11] Barber B P and Putterman S J 1992 *Phys. Rev. Lett.* **69** 3839
- [12] Hiller R, Weninger K, Putterman S J and Barber B P 1994 *Science* **266** 248
- [13] Brenner M P, Hilgenfeldt S and Lohse D 2002 *Rev. Mod. Phys.* **74** 425
- [14] Lohse D, *Nature* 2002 **418** 381
- [15] Flannigan D J and Suslick K S 2005 *Nature* **434** 52
- [16] Suslick K S and Flannigan D J 2008 *Annu. Rev. Phys. Chem.* **59** 659
- [17] Kurcz A, Capolupo A and Beige A 2009 *New J. Phys.* **11** 053001
- [18] Xu H X and Suslick K S 2010 *Phys. Rev. Lett.* **104** 244301-1-4
- [19] Flannigan D J and Suslick K S 2010 *Nature Physics* **6** 598-601
- [20] Tari A 2003 *The Specific Heat of Matter at Low Temperatures*, (London: Imperial College Press)
- [21] Zeldovich Y B and Raizer Y P 1966 *Physics of shock waves and high-temperature hydrodynamic phenomena, Vols. I and II*, (New York: Academic Press)